AMERICAN SOCIETY FOR MICROBIOLOGY | Journal of Bacteriology®

RESEARCH ARTICLE

Hypoxanthine-Guanine Phosphoribosyltransferase Is Dispensable for *Mycobacterium smegmatis* Viability

Zdeněk Knejzlík,[a] Klára Herkommerová,[a] Dana Hocková,[a] Iva Pichová[a]

[a]Institute of Organic Chemistry and Biochemistry of the Czech Academy of Sciences, Prague, Czech Republic

ABSTRACT Purine metabolism plays a ubiquitous role in the physiology of *Mycobacterium tuberculosis* and other mycobacteria. The purine salvage enzyme hypoxanthine-guanine phosphoribosyltransferase (HGPRT) is essential for *M. tuberculosis* growth *in vitro*; however, its precise role in *M. tuberculosis* physiology is unclear. Membrane-permeable prodrugs of specifically designed HGPRT inhibitors arrest the growth of *M. tuberculosis* and represent potential new antituberculosis compounds. Here, we investigated the purine salvage pathway in the model organism *Mycobacterium smegmatis*. Using genomic deletion analysis, we confirmed that HGPRT is the only guanine and hypoxanthine salvage enzyme in *M. smegmatis* but is not required for *in vitro* growth of this mycobacterium or survival under long-term stationary-phase conditions. We also found that prodrugs of *M. tuberculosis* HGPRT inhibitors displayed an unexpected antimicrobial activity against *M. smegmatis* that is independent of HGPRT. Our data point to a different mode of mechanism of action for these inhibitors than was originally proposed.

IMPORTANCE Purine bases, released by the hydrolytic and phosphorolytic degradation of nucleic acids and nucleotides, can be salvaged and recycled. The hypoxanthine-guanine phosphoribosyltransferase (HGPRT), which catalyzes the formation of guanosine-5′-monophosphate from guanine and inosine-5′-monophosphate from hypoxanthine, represents a potential target for specific inhibitor development. Deletion of the HGPRT gene (Δ*hgprt*) in the model organism *Mycobacterium smegmatis* confirmed that this enzyme is not essential for *M. smegmatis* growth. Prodrugs of acyclic nucleoside phosphonates (ANPs), originally designed against HGPRT from *Mycobacterium tuberculosis*, displayed anti-*M. smegmatis* activities comparable to those obtained for *M. tuberculosis* but also inhibited the Δ*hgprt M. smegmatis* strain. These results confirmed that ANPs act in *M. smegmatis* by a mechanism independent of HGPRT.

KEYWORDS purine salvage pathway, hypoxanthine-guanine phosphoribosyltransferase, guanine, hypoxanthine, *Mycobacterium smegmatis*, inhibitors

Mycobacterium tuberculosis is an opportunistic pathogen that caused 1.2 million deaths among HIV-negative people worldwide in 2018 and an additional 251,000 deaths among people with HIV (1). The evolution of *M. tuberculosis* strains with resistance to multiple first- and second-line drugs (2) has led to an urgent need for new types of antituberculosis compounds. Purine metabolism plays a ubiquitous role in the physiology of mycobacteria, which are able to both synthesize purines *de novo* and scavenge them via the salvage pathway (3–5). Inhibitors targeting several enzymes implicated in purine metabolism can suppress *M. tuberculosis* growth at micromolar concentrations (6–12).

Hypoxanthine-guanine phosphoribosyltransferase (HGPRT; EC 2.4.2.8), the key enzyme in the purine salvage pathway, catalyzes the synthesis of inosine- or guanosine-5′-monophosphate via replacement of the 1-pyrophosphate group in phosphoribosyl

Citation Knejzlík Z, Herkommerová K, Hocková D, Pichová I. 2020. Hypoxanthine-guanine phosphoribosyltransferase is dispensable for *Mycobacterium smegmatis* viability. J Bacteriol 202:e00710-19. https://doi.org/10.1128/JB.00710-19.

Editor Anke Becker, Philipps-Universität Marburg

Address correspondence to Iva Pichová, iva.pichova@uochb.cas.cz.

Received 19 November 2019
Accepted 5 December 2019
Accepted manuscript posted online 9 December 2019
Published 11 February 2020

pyrophosphate with a corresponding free nucleobase. Its precise role in *M. tuberculosis* physiology remains unclear due to a lack of sufficient experimental data; however, based on random saturation insertional mutagenesis analysis, HGPRT has been proposed to be essential for *M. tuberculosis* growth *in vitro* (13, 14). A detailed enzymatic mechanism and oligomerization analysis revealed that *M. tuberculosis* HGPRT belongs to the type I phosphoribosyltransferase family (15, 16). The arrangement of the sequentially unique mobile loop in the *M. tuberculosis* HGPRT molecule is responsible for its distinct kinetic properties and quaternary structure organization compared to its human counterpart (12, 15). In the *M. tuberculosis* HGPRT structure, these loops are located between the subunits of tetramers, whereas in the human HGPRT structure, the loops are at the extremities of the tetramer. This difference enabled the design of acyclic nucleoside phosphonate (ANP) inhibitors—analogues of natural nucleotides (17) with high selectivity for *M. tuberculosis* HGPRT over its human counterpart. The corresponding cell membrane-permeable phosphoramidate prodrugs inhibited *M. tuberculosis* growth *in vitro* at micromolar concentrations (12). However, the detailed mechanism of antibacterial activity of these prodrugs has not been studied in detail.

Mycobacterium smegmatis is a fast-growing saprophytic bacteria often used as a model in mycobacterial research because it shares many basic features with *M. tuberculosis*, such as cell wall biogenesis, adaptation to low oxygen conditions, dormancy, and stress response (18). Locus MSMEG_6110 in the *M. smegmatis* genome encodes a HGPRT that shares 85% primary sequence homology with its *M. tuberculosis* counterpart. Conservation of amino acid residues involved in the binding of substrates and ANP-based inhibitors suggests similar modes of action for the *M. tuberculosis* and *M. smegmatis* HGPRT homologues (12).

In this study, we examined the role of HGPRT in *M. smegmatis* and found that *M. smegmatis* growth is unexpectedly sensitive to treatment with ANP phosphoramidate prodrugs independently on HGPRT.

RESULTS

HGPRT is not essential for *M. smegmatis* growth. To analyze the importance of HGPRT for *M. smegmatis* growth, we deleted the HGPRT coding sequence (Δ*hgprt*) using the method described by Shenkerman et al. (2014) (19). Briefly, this involved Chec9 DNA recombinase-directed gene knockout with a pYS2 plasmid-derived deletion Hyg^r cassette flanked by 32-bp *loxP* sites, which allows precise recombination of DNA sequences of interest and subsequent excision of the cassette from the chromosome by a Cre recombinase mediated by *loxP* sites. Colonies of recombinants, selected on agar medium with hygromycin, were visible after 3 days of cultivation. The resulting genetic background of the *M. smegmatis* Δ*hgprt* strain was verified by PCR using specific primers that anneal close to the upstream and downstream 700-bp recombination regions (Fig. 1A). PCR with the wild-type (wt) strain, used as a reference, yielded an amplicon of 2,089 bp (Fig. 1B), corresponding to the HGPRT coding sequence and upstream and downstream regions (Fig. 1A). The Δ*hgprt* strain amplicon was 1,539 bp (Fig. 1B), indicating that the 582-bp HGPRT coding sequence had been replaced with the 32-bp *loxP* site (Fig. 1A). DNA sequencing of the 1,539-bp amplicon confirmed the expected recombination process. We also carried out a control PCR using primers specific for the HGPRT gene to confirm the absence of the HGPRT coding sequence in different genome positions of the Δ*hgprt* strain. We used primers specific for the adenine phosphoribosyltransferase (APRT) gene as a positive control. Both HGPRT and APRT amplicons were generated in PCRs with the reference wt strain, while only the APRT amplicon was present in reactions with the Δ*hgprt* strain (Fig. 1C and D).

To assess the Δ*hgprt* strain phenotype, the wt and mutated strain were grown on solid minimal Hartmans-De Bont (HdB) medium or Middlebrook 7H10–albumin-dextrose complex (7H10-ADC) medium. Growth (Fig. 2A) and survival under the stationary phase (Fig. 2B) were comparable for the wt and Δ*hgprt* strains, confirming that

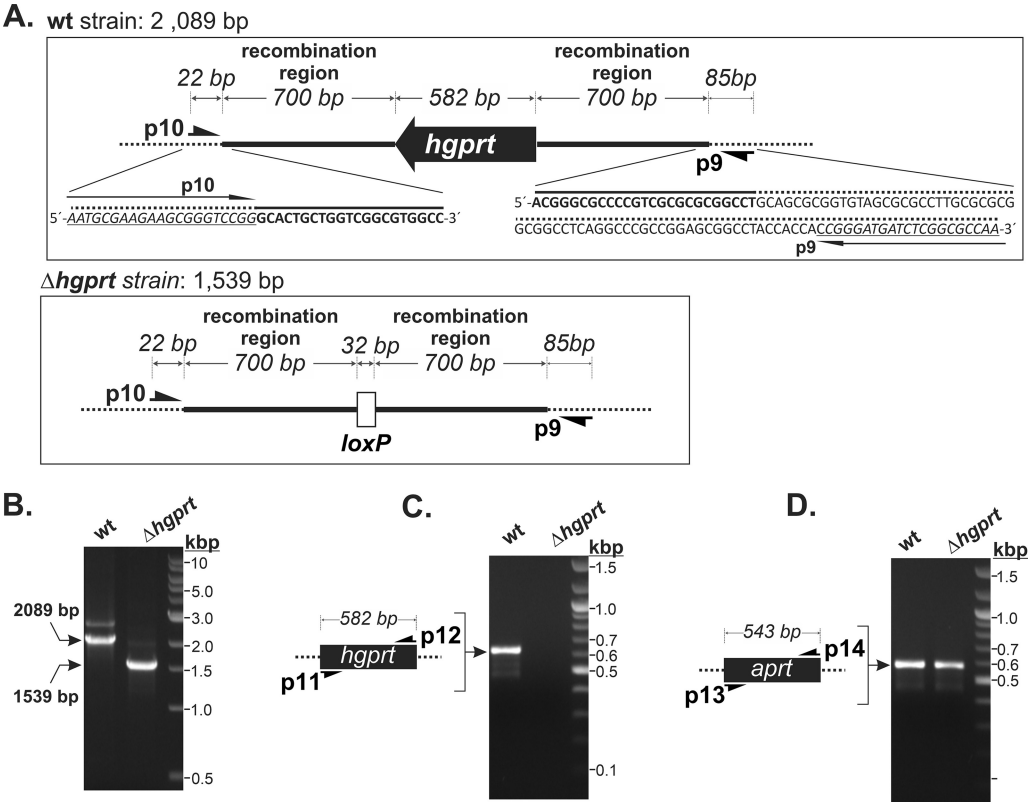

FIG 1 PCR screening of the HGPRT coding sequence deletion. (A) Schematic showing the HGPRT gene region in the wt strain (top panel) and its replacement with the 32-bp loxP site in the Δ*hgprt* strain (bottom panel). The bold line corresponds to the 700-bp upstream and downstream HGPRT gene regions used for homologous recombination with the hygromycin cassette (Hyg^r). Positions of screening primers p9 and p10 are indicated (B to D). Chromosomal DNA from wt and Δ*hgprt* strains was isolated and used as the templates for independent PCR experiments using the following primer pairs: p9/p10, which anneal in the boundaries of the recombined region (B); p11/p12, which are specific for the HGPRT coding sequence (C); and p13/p14, which are specific for the APRT coding sequence (used as a positive control) (D). Samples were separated on 1% agarose gels.

HGPRT is not essential for *M. smegmatis* growth. The data also suggest that HGPRT does not contribute to adaptation to long-term starvation conditions (Fig. 2B).

Guanine/hypoxanthine salvage is catalyzed exclusively by HGPRT in *M. smegmatis*. We next tested the importance of HGPRT for the salvage of adenine, guanine, and hypoxanthine. To impair *de novo* biosynthesis of purine bases and direct purine metabolism through the salvage pathway, we knocked out amidophosphoribosyltransferase (PurF) (20, 21), which catalyzes the first step of *de novo* purine synthesis. Additionally, we

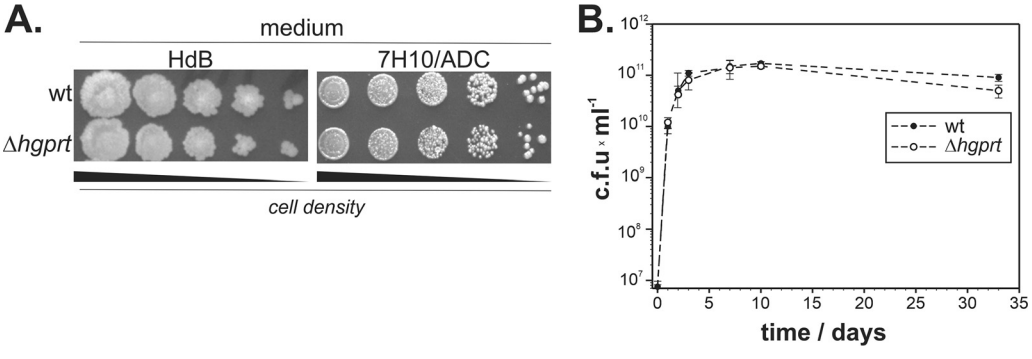

FIG 2 Influence of HGPRT deletion on *M. smegmatis* growth. (A) Growth of the wt and Δ*hgprt* strains on minimal HdB and 7H10-ADC (28) solid media; (B) bacterial survival during the stationary phase in 7H9-ADC medium.

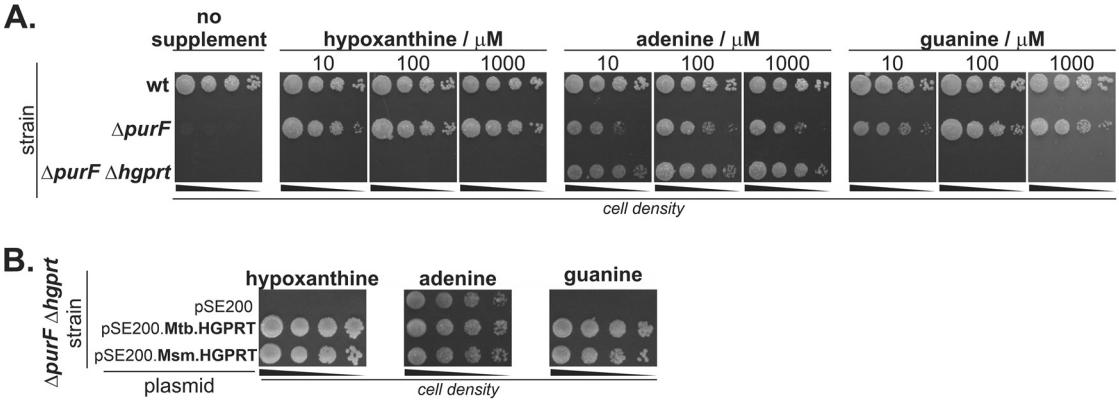

FIG 3 Role of HGPRT in the *M. smegmatis* purine salvage pathway. (A) Effect of inactivation of the *purF* coding sequence on wt and Δ*hgprt M. smegmatis* purine auxotrophy. *M. smegmatis* strains were grown on 7H10-ADC medium with or without purine supplement at indicated concentrations for 3 days at 37°C. (B) Plasmid-based complementation of HGPRT activity in the Δ*purF* Δ*hgprt* strain. Bacteria transformed with empty vector (pSE200) or vectors carrying *M. tuberculosis*/*M. smegmatis* HGPRT coding sequences were cultivated on 7H10-ADC with 25 μg/ml kanamycin and 100 μM purine supplement for 3 days at 37°C.

prepared the Δ*purF* Δ*hgprt* double mutant. We compared the growth of the wt, Δ*hgprt*, Δ*purF*, and Δ*purF* Δ*hgprt* strains on solid medium in the presence of hypoxanthine, adenine, and guanine. As was reported previously (21), the Δ*purF M. smegmatis* strain was unable to grow in the absence of a purine supplement, and its growth was restored in the presence of hypoxanthine, adenine, or guanine at concentration higher than 10 μM (Fig. 3A). Growth of the Δ*purF* Δ*hgprt* mutant, with simultaneously inactivated *de novo* purine biosynthesis and HGPRT activity, was observed only in the presence of adenine (Fig. 3A). To confirm the role of HGPRT in *M. smegmatis* purine biosynthesis and to assess whether *M. tuberculosis* HGPRT has similar properties, we performed complementation experiments in the *M. smegmatis* Δ*purF* Δ*hgprt* strain using plasmids expressing *M. smegmatis* and *M. tuberculosis* HGPRTs. Growth of the strain was restored by both *M. smegmatis* and *M. tuberculosis* HGPRT enzymes (Fig. 3B). Our results indicate that HGPRT is the exclusive salvaging enzyme for guanine and hypoxanthine in *M. smegmatis* and suggest that *M. tuberculosis* HGPRT behaves similarly.

ANP-based inhibitors of *M. tuberculosis* HGPRT arrest *M. smegmatis* growth but do not target *M. smegmatis* HGPRT. The amino acid sequences of HGPRT from *M. smegmatis* and *M. tuberculosis* share 72% identity and 85% similarity, and the residues forming binding pockets for purines, pyrophosphate, and the Mg^{2+} cation are conserved (Fig. 4A). We built a model of the *M. smegmatis* HGPRT structure (Fig. 4B) using the structure of *M. tuberculosis* HGPRT in complex with inhibitor 9 (Fig. 4D), a guanine-derived double-branched ANP, as the template (12). The overall model (Fig. 4B) and detail of the active site (Fig. 4C) suggest identical binding of this compound to *M. smegmatis* HGPRT.

Eng et al. (12) previously reported that membrane-permeable phosphoramidate prodrugs, derived from corresponding acyclic nucleoside phosphonates, selectively inhibit purified *M. tuberculosis* HGPRT and arrest *M. tuberculosis* growth. We tested two prodrugs from a series previously prepared in our laboratory, the tetraphosphoramidate compound 30 (prodrug of 9; MIC_{50} of 4.5 μM for *M. tuberculosis* strain H37Rv) (Fig. 4D) and the corresponding hypoxanthine derivative 31 (prodrug of 10, MIC_{50} of 8 μM for *M. tuberculosis*), for growth arrest of wt and mutant *M. smegmatis* (Table 1). Both compounds had MIC_{50} values for wt *M. smegmatis* comparable to those obtained for *M. tuberculosis*, but surprisingly, they also comparably inhibited the Δ*hgprt* strain and the Δ*purF* strain, which are dependent on HGPRT activity and can grow only in the presence of purines. Because the solubility of guanine in the cultivation media used in this study is limited, we cultivated the Δ*purF* strain in the presence of hypoxanthine (Table 1). Overexpression of both *M. tuberculosis* and *M. smegmatis* HGPRT enzymes in the wt and Δ*purF* Δ*hgprt M. smegmatis* strains did not change the

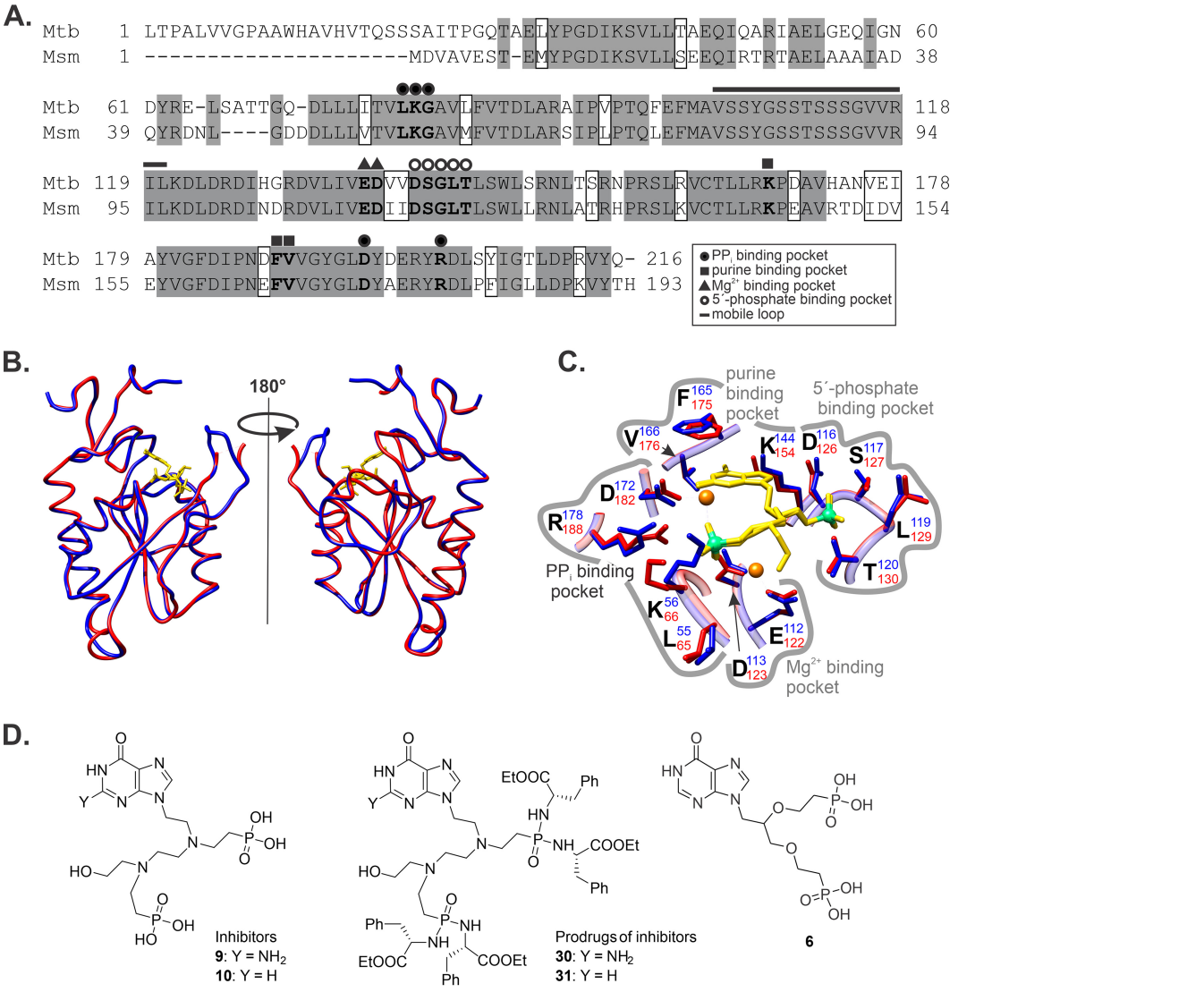

FIG 4 Similarity of *M. smegmatis* and *M. tuberculosis* HGPRTs. (A) *M. tuberculosis* and *M. smegmatis* HGPRT primary structure alignment. Identical and similar amino acid residues are in gray and white boxes, respectively. Key amino acid residues involved in binding of double-branched ANPs are in bold. (B) Structural model of *M. smegmatis* HGPRT (blue) aligned with *M. tuberculosis* HGPRT in complex with compound 9 (red; PDB code 4RHX), which was used as a template. Compound 9 is shown in yellow. (C) Active site of *M. tuberculosis* HGPRT (red) and the *M. smegmatis* HGPRT model (blue) in complex with compound 9 (yellow). Key amino acid residues involved in the binding are shown. (D) Structures of ANP inhibitors and their prodrugs (12).

MIC_{50} value. These unexpected results indicate that both inhibitors target another protein, the function of which is crucial for *M. smegmatis* viability.

DISCUSSION

In this study, we showed that HGPRT is the only guanine/hypoxanthine salvage enzyme in *M. smegmatis*, but its activity is not required for viability under standard growth conditions. We also found that prodrugs derived from ANP-based inhibitors designed for the highly similar *M. tuberculosis* HGPRT do not target *M. smegmatis* HGPRT but display antimicrobial activity against *M. smegmatis*. This finding raises questions about the selectivity of known *M. tuberculosis* HGPRT-targeted compounds in bacterial cells (12). A random genome phage mutagenesis screen of *M. tuberculosis* (13, 14) identified HGPRT as an essential gene for *M. tuberculosis*; however, the phenotype of the Δ*hgprt M. tuberculosis* strain has not been analyzed. Previous characterizations of *M. tuberculosis* HGPRT emphasized the necessity of evaluating the Δ*hgprt M. tubercu-*

TABLE 1 MIC_{50} values of prodrugs of acyclic nucleoside phosphonate *M. tuberculosis* HGPRT inhibitors

Species and strain	Plasmid	MIC_{50} ± SD (μM) of compound: 30	31
M. tuberculosis[a] H37Rv	None	4.5	8.0
M. smegmatis			
wt	None	8.1 ± 0.4	15.6 ± 0.9
	None	8.1 ± 0.6 (Hpx)[b]	16.1 ± 1.8 (Hpx)
	pSE200-Mtb.HGPRT	8.2 ± 0.9	13.9 ± 1.7
	pSE200-Msm.HGPRT	8.3 ± 0.6	13.6 ± 1.9
Δ*hgprt* strain	None	8.0 ± 0.9	15.6 ± 1.1
Δ*purF* strain	None	8.9 ± 1.2 (Hpx)	22.2 ± 2.4 (Hpx)
Δ*purF* Δ*hgprt* strain	pSE200-Mtb.HGPRT	8.7 ± 0.7 (Hpx)	20.1 ± 2.2 (Hpx)
	pSE200-Msm.HGPRT	8.8 ± 0.5 (Hpx)	19.2 ± 3 (Hpx)

[a]Published in reference 12.
[b]Hpx, in the presence of 100 μM hypoxanthine.

losis phenotype to elucidate the exact role of HGPRT in *M. tuberculosis* physiology and metabolic changes during the transition to hypoxia (16).

Eng and coworkers presented the first crystal structures of *M. tuberculosis* HGPRT in complex with ANP-based compounds that inhibit the enzyme at micromolar concentrations (PDB codes 4RHU, 4RHX, and 4RHY), revealing that these compounds fit well in the active site (12). These micromolar inhibitors did not display any significant antimicrobial activities because their highly polar character does not allow them to cross cell membranes. However, using a prodrug approach (22) to mask the charges of the phosphonate moieties by attaching hydrophobic groups via a phosphoramidate bond facilitated penetration of these compounds into *M. tuberculosis* and improved their antimicrobial activities. Notably, protein target analysis of synthesized prodrugs in *M. tuberculosis* has not been performed. Interestingly, the MIC_{50} values of these compounds for *M. tuberculosis* growth were in the 4.5 to 15 μM range, even for compound 6 (Fig. 4D), which displayed very low inhibitory activity in enzymatic tests (K_i, ≥50 μM) (12). Our aim was not to test ANPs for *in vitro* inhibition of an isolated *M. smegmatis* enzyme but to use the constructed *M. smegmatis* HGPRT knockout mutants to analyze the selectivity of HGPRT inhibitors in bacterial cells. The model of the complex of compound 9 with *M. smegmatis* HGPRT (Fig. 4B), based on the structure of *M. tuberculosis* HGPRT with this inhibitor (K_i, 1.6 μM), showed enzyme-inhibitor interactions identical to those observed in *M. tuberculosis* HGPRT (Fig. 4C), suggesting similar inhibition activities. Assays of the antimicrobial activity of guanine- and hypoxanthine-containing prodrugs (compounds 30 and 31, respectively) against *M. smegmatis* resulted in MIC_{50} values comparable to those obtained for *M. tuberculosis*. However, we obtained comparable MIC_{50} values for the Δ*hgprt*, Δ*purF*, and Δ*purF* Δ*hgprt M. smegmatis* strains in the presence of overexpressed *M. smegmatis* HGPRT, indicating thatj the antimicrobial activity of ANP prodrugs is not attributable to inhibition of HGPRT.j Rather, the compounds act by a different mechanism than originally supposed. The unchanged MIC_{50} values of 30 and 31 in wt *M. smegmatis* in the presence of overexpressed *M. tuberculosis* HGPRT suggest that a similar mechanism also functions in *M. tuberculosis*.

We cannot rule out differences in purine metabolism and the role of HGPRT in *M. smegmatis* and *M. tuberculosis*, as purine salvage pathways and the biosynthesis of nucleic acids have not been investigated in detail in both species. Furthermore, adaptation to different ecological niches could be responsible for many metabolic differences (23). Our data, however, show that inhibitors designed and tested against particular intracellular mycobacterial enzymes can have a different-than-expected mode of action, suggesting that their mechanisms in bacterial cells must be evaluated in more detail.

TABLE 2 List of *M. smegmatis* strains used in this study

Strain genotype	Parental strain/genotype	Reference
wt	mc^2 155/wt	29
Δ*hgprt*	mc^2 155/*hgprt*::*loxP*	This study
Δ*purF*	mc^2 155/*purF*::Hyg^r	This study
Δ*hgpr* Δ*purF*	Δ*hgprt*/*hgprt*::*loxP purF*::Hyg^r	This study

MATERIALS AND METHODS

Construction of plasmids. pYS2-based deletion plasmids (19) were constructed as follows: regions of amplified sequences and corresponding primers used to construct pYS2-based deletion plasmids are listed in Table S1 in the supplemental material. Upstream (*ups*) and downstream (*dns*) regions of the *hgprt* and *purF* coding sequences were amplified by PCR using Q5 DNA polymerase (New England BioLabs) with *M. smegmatis* chromosomal DNA as the template. *ups* regions were inserted into pYS2 via SpeI and SwaI sites using T4 DNA ligase and were sequenced. Similarly, the corresponding *dns* region sequences were inserted into the pYS2 intermediates via PacI and NsiI sites. The pSE200-based constitutive expression plasmids (21) were constructed as follows: *M. tuberculosis Mtb.hgprt* and *M. smegmatis Msm.hgprt* were PCR amplified from corresponding template chromosomal DNA using primer pairs 15/16 and 17/18, respectively. PCR fragments were inserted into SwaI-linearized pSE200 using the In-Fusion approach. All prepared constructs were verified by sequencing. *M. smegmatis* strains were transformed as previously described (24). Primers are listed in Table S1.

Gene deletion. Gene disruption using a pYS2 deletion plasmid has been described previously (19). Briefly, *M. smegmatis* carrying the temperature-sensitive replicating expression plasmid pYS1 encoding Chec9 DNA recombinase under the control of the acetamidase promoter was inoculated in 7H9-ADC medium containing 25 μg/ml kanamycin and 0.25% acetamide to an initial optical density at 600 nm (OD_{600}) of 0.001. The culture was grown at 34°C and 220 rpm until the OD_{600} reached 0.8. The culture was then used for preparation of competent cells, which were transformed with a PacI-linearized pYS2 deletion plasmid (24). Gene disruptants were selected on 7H10-ADC medium containing 150 μg/ml hygromycin at 42°C to cure out of the pYS1 vector. To remove the Hyg^r cassette, gene disruptants were next transformed with the pML2714 vector, which constitutively expresses Cre recombinase. In the resulting gene disruptants, the deleted gene was replaced with a 32-bp *loxP* site. Deletions were screened by PCR using Q5 polymerase and primer pairs that anneal at the boundaries of the deleted region (Table S1 and Fig. 1). The resulting PCR product was sequenced. Constructed *M. smegmatis* deletion strains are listed in Table 2.

Synthesis of ANP phosphoramidate prodrugs 30 and 31. Prodrugs of ANP-based inhibitors were prepared as previously described (12). Characterization of synthetic compounds is described in the supplemental material. The samples tested on *M. smegmatis* were identical to those tested previously on *M. tuberculosis*.

Determination of antibacterial activities of ANP prodrugs. *M. smegmatis* strains were propagated in 7H9-ADC medium containing 0.5% (vol/vol) glycerol and 0.05% tyloxapol to the mid-exponential phase (OD_{600} of 0.5). When required, 100 μM hypoxanthine was additionally present. Strains carrying pSE200-based expression vectors were cultivated in the presence of 25 μg/ml kanamycin. This culture was used to test the antimicrobial activity of ANP prodrugs with a modified resazurin microplate assay (25). Serially diluted ANP prodrugs in 7H9-ADC medium containing 0.05% tyloxapol and 0.5% glycerol were pipetted in 100-μl aliquots into a 96-well plate, and the final concentration of dimethyl sulfoxide (DMSO) was adjusted to 0.5%. *M. smegmatis* culture at an OD_{600} of 0.005 (100 μl) was added. Plates were incubated at 37°C for 24 h, 30 μl of a 0.02% resazurin solution in phosphate-buffered saline (PBS) was added, and the plate was incubated for an additional 24 h. Sample fluorescence was determined with a Tecan Infinite M1000 microplate reader with an excitation wavelength of 530 nm and emission read at 580 nm. Growth was calculated as follows:

$$\%\ \text{of growth} = \frac{\text{FL(sample)} - \text{FL(blank)}}{\text{FL(positive control)} - \text{FL(blank)}} \times 100$$

where FL(positive control) represents a *M. smegmatis* culture sample, without ANPs and FL(blank) represents cultivation without cells.

Stationary-phase survival assay. *M. smegmatis* was inoculated into 100 ml of 7H9-ADC medium with 0.5% (vol/vol) glycerol and 0.05% tyloxapol to an OD_{600} of 0.005 in a 500-ml Erlenmeyer flask. Cultures were cultivated at 37°C and 180 rpm. Aliquots (1 ml) were collected at 0, 1, 3, 5, 7, 10, and 31 days of cultivation and serially diluted. A 30-μl aliquot of each dilution was spotted onto 7H10-ADC plates. Plates were incubated for 3 days at 37°C, and CFUs were determined from spots with 10 to 40 *M. smegmatis* colonies.

***M. smegmatis* cultivation on agar media.** *M. smegmatis* strains were cultivated in 7H9-ADC medium with medium containing 0.5% (vol/vol) glycerol and 0.05% tyloxapol until cultures reached the mid-exponential growth phase. When required, cultures were supplemented with 100 μM hypoxanthine or 25 μg/ml kanamycin. Cells were pelleted at 3,000 × *g* for 5 min and washed twice with PBS. The final OD_{600} was adjusted to 0.1, and three serial 10-fold dilutions were prepared. Fractions from these dilutions (5 μl) were spotted onto 7H10-ADC medium containing 0.5% glycerol; 3 mM asparagine; and 200 μM adenine, guanine, or hypoxanthine. Growth was compared with that on purine-free medium.

To test complementation of HGPRT deficiency in the Δ*purF* Δ*hgprt* strain, the bacteria were transformed with pSE200.Mtb.HGPRT, pSE200.Msm.HGPRT, or empty pSE200 and selected on 7H10-ADC medium containing 25 μg/ml kanamycin, 100 μM adenine, and 3 mM asparagine. Resulting transformants were spotted onto 7H10-ADC containing 25 μg/ml kanamycin and 100 μM adenine, hypoxanthine, or guanine.

Sequence alignment and 3D modeling. Alignment of *M. tuberculosis* and *M. smegmatis* HGPRT amino acid sequences was performed with Clustal W. The structural model of *M. smegmatis* HGPRT was built with UCSF Chimera with the Modeller software extension (26, 27) using the *M. tuberculosis* HGPRT X-ray structure as a template (PDB 4RHX) (12).

SUPPLEMENTAL MATERIAL

Supplemental material is available online only.

SUPPLEMENTAL FILE 1, PDF file, 1.6 MB.

ACKNOWLEDGMENTS

This work was supported by the Ministry of Education of the Czech Republic (NPU I LO 1302).

We thank Dagmar Grundová for excellent technical support.

We declare that we have no conflict of interest.

REFERENCES

1. World Health Organization. 2019. Global tuberculosis report 2019. World Health Organization, Geneva, Switzerland. https://www.who.int/tb/publications/global_report/en/.
2. Daley CL, Caminero JA. 2018. Management of multidrug-resistant tuberculosis. Semin Respir Crit Care Med 39:310–324. https://doi.org/10.1055/s-0038-1661383.
3. Wheeler PR. 1987. Biosynthesis and scavenging of purines by pathogenic mycobacteria including *Mycobacterium leprae*. J Gen Microbiol 133:2999–3011. https://doi.org/10.1099/00221287-133-11-2999.
4. Malathi VG, Ramakrishnan T. 1966. Biosynthesis of nucleic acid purines in *Mycobacterium tuberculosis* H37Rv. Biochem J 98:594–597. https://doi.org/10.1042/bj0980594.
5. Ducati RG, Breda A, Basso LA, Santos DS. 2011. Purine salvage pathway in *Mycobacterium tuberculosis*. Curr Med Chem 18:1258–1275. https://doi.org/10.2174/092986711795029627.
6. Parker WB, Long MC. 2007. Purine metabolism in *Mycobacterium tuberculosis* as a target for drug development. Curr Pharm Des 13:599–608. https://doi.org/10.2174/138161207780162863.
7. Makowska-Grzyska M, Kim Y, Gorla SK, Wei Y, Mandapati K, Zhang M, Maltseva N, Modi G, Boshoff HI, Gu M, Aldrich C, Cuny GD, Hedstrom L, Joachimiak A. 2015. *Mycobacterium tuberculosis* IMPDH in complexes with substrates, products and antitubercular compounds. PLoS One 10:e0138976. https://doi.org/10.1371/journal.pone.0138976.
8. Usha V, Gurcha SS, Lovering AL, Lloyd AJ, Papaemmanouil A, Reynolds RC, Besra GS. 2011. Identification of novel diphenyl urea inhibitors of Mt-GuaB2 active against *Mycobacterium tuberculosis*. Microbiology 157:290–299. https://doi.org/10.1099/mic.0.042549-0.
9. Park Y, Pacitto A, Bayliss T, Cleghorn LAT, Wang Z, Hartman T, Arora K, Ioerger TR, Sacchettini J, Rizzi M, Donini S, Blundell TL, Ascher DB, Rhee K, Breda A, Zhou N, Dartois V, Jonnala SR, Via LE, Mizrahi V, Epemolu O, Stojanovski L, Simeons F, Osuna-Cabello M, Ellis L, MacKenzie CJ, Smith ARC, Davis SH, Murugesan D, Buchanan KI, Turner PA, Huggett M, Zuccotto F, Rebollo-Lopez MJ, Lafuente-Monasterio MJ, Sanz O, Diaz GS, Lelièvre J, Ballell L, Selenski C, Axtman M, Ghidelli-Disse S, Pflaumer H, Bösche M, Drewes G, Freiberg GM, Kurnick MD, Srikumaran M, Kempf DJ, Green SR, Ray PC, Read K, Wyatt P, Barry CE, Boshoff HI. 2017. Essential but not vulnerable: indazole sulfonamides targeting inosine monophosphate dehydrogenase as potential leads against *Mycobacterium tuberculosis*. ACS Infect Dis 3:18–33. https://doi.org/10.1021/acsinfecdis.6b00103.
10. Keough DT, Hockova D, Rejman D, Spacek P, Vrbkova S, Krecmerova M, Eng WS, Jans H, West NP, Naesens LMJ, de Jersey J, Guddat LW. 2013. Inhibition of the *Escherichia coli* 6-oxopurine phosphoribosyltransferases by nucleoside phosphonates: potential for new antibacterial agents. J Med Chem 56:6967–6984. https://doi.org/10.1021/jm400779n.
11. Eng WS, Rejman D, Pohl R, West NP, Woods K, Naesens LMJ, Keough DT, Guddat LW. 2018. Pyrrolidine nucleoside bisphosphonates as antituberculosis agents targeting hypoxanthine-guanine phosphoribosyltransferase. Eur J Med Chem 159:10–22. https://doi.org/10.1016/j.ejmech.2018.09.039.
12. Eng WS, Hockova D, Spacek P, Janeba Z, West NP, Woods K, Naesens LMJ, Keough DT, Guddat LW. 2015. First crystal structures of *Mycobacterium tuberculosis* 6-oxopurine phosphoribosyltransferase: complexes with GMP and pyrophosphate and with acyclic nucleoside phosphonates whose prodrugs have antituberculosis activity. J Med Chem 58:4822–4838. https://doi.org/10.1021/acs.jmedchem.5b00611.
13. Griffin JE, Gawronski JD, DeJesus MA, Ioerger TR, Akerley BJ, Sassetti CM. 2011. High-resolution phenotypic profiling defines genes essential for mycobacterial growth and cholesterol catabolism. PLoS Pathog 7:e1002251. https://doi.org/10.1371/journal.ppat.1002251.
14. DeJesus MA, Gerrick ER, Xu WZ, Park SW, Long JE, Boutte CC, Rubin EJ, Schnappinger D, Ehrt S, Fortune SM, Sassetti CM, Ioerger TR. 2017. Comprehensive essentiality analysis of the *Mycobacterium tuberculosis* genome via saturating transposon mutagenesis. mBio 8:e02133-16. https://doi.org/10.1128/mBio.02133-16.
15. Eng WS, Keough DT, Hockova D, Winzor DJ, Guddat LW. 2017. Oligomeric state of hypoxanthine-guanine phosphoribosyltransferase from *Mycobacterium tuberculosis*. Biochimie 135:6–14. https://doi.org/10.1016/j.biochi.2016.12.020.
16. Patta PC, Martinelli LKB, Rotta M, Abbadi BL, Santos DS, Basso LA. 2015. Mode of action of recombinant hypoxanthine-guanine phosphoribosyltransferase from *Mycobacterium tuberculosis*. RSC Adv 5:74671–74683. https://doi.org/10.1039/C5RA14918E.
17. Keough DT, Hockova D, Holy A, Naesens LMJ, Skinner-Adams TS, de Jersey J, Guddat LW. 2009. Inhibition of hypoxanthine-guanine phosphoribosyltransferase by acyclic nucleoside phosphonates: a new class of antimalarial therapeutics. J Med Chem 52:4391–4399. https://doi.org/10.1021/jm900267n.
18. Tyagi JS, Sharma D. 2002. *Mycobacterium smegmatis* and tuberculosis. Trends Microbiol 10:68–69. https://doi.org/10.1016/s0966-842x(01)02296-x.
19. Shenkerman Y, Elharar Y, Vishkautzan M, Gur E. 2014. Efficient and simple generation of unmarked gene deletions in *Mycobacterium smegmatis*. Gene 533:374–378. https://doi.org/10.1016/j.gene.2013.09.082.
20. Keer J, Smeulders MJ, Williams HD. 2001. A *purF* mutant of *Mycobacterium smegmatis* has impaired survival during oxygen-starved stationary phase. Microbiology 147:473–481. https://doi.org/10.1099/00221287-147-2-473.
21. Knejzlik Z, Herkommerova K, Pichova I. 2019. Catabolism of 8-oxopurines is mainly routed via the guanine to xanthine interconversion pathway in *Mycobacterium smegmatis*. Tuberculosis (Edinb) 119:101879. https://doi.org/10.1016/j.tube.2019.101879.
22. Hockova D, Janeba Z, Naesens L, Edstein MD, Chavchich M, Keough DT, Guddat LW. 2015. Antimalarial activity of prodrugs of N-branched acyclic nucleoside phosphonate inhibitors of 6-oxopurine phosphoribosyltrans-

ferases. Bioorg Med Chem 23:5502–5510. https://doi.org/10.1016/j.bmc.2015.07.038.
23. Banuls A-L, Sanou A, Anh NTV, Godreuil S. 2015. *Mycobacterium tuberculosis*: ecology and evolution of a human bacterium. J Med Microbiol 64:1261–1269. https://doi.org/10.1099/jmm.0.000171.
24. Goude R, Roberts DM, Parish T. 2015. Electroporation of mycobacteria. Methods Mol Biol 1285:117–130. https://doi.org/10.1007/978-1-4939-2450-9_7.
25. Blanco-Ruano D, Roberts DM, Gonzalez-Del-Rio R, Álvarez D, Rebollo MJ, Pérez-Herrán E, Mendoza A. 2015. Antimicrobial susceptibility testing for *Mycobacterium sp*. Methods Mol Biol 1285:257–268. https://doi.org/10.1007/978-1-4939-2450-9_15.
26. Pettersen EF, Goddard TD, Huang CC, Couch GS, Greenblatt DM, Meng EC, Ferrin TE. 2004. UCSF Chimera—a visualization system for exploratory research and analysis. J Comput Chem 25:1605–1612. https://doi.org/10.1002/jcc.20084.
27. Šali A, Blundell TL. 1993. Comparative protein modelling by satisfaction of spatial restraints. J Mol Biol 234:779–815. https://doi.org/10.1006/jmbi.1993.1626.
28. Berney M, Weimar MR, Heikal A, Cook GM. 2012. Regulation of proline metabolism in mycobacteria and its role in carbon metabolism under hypoxia. Mol Microbiol 84:664–681. https://doi.org/10.1111/j.1365-2958.2012.08053.x.
29. Snapper SB, Melton RE, Mustafa S, Kieser T, Jacobs WR, Jr. 1990. Isolation and characterization of efficient plasmid transformation mutants of *Mycobacterium smegmatis*. Mol Microbiol 4:1911–1919. https://doi.org/10.1111/j.1365-2958.1990.tb02040.x.